Fluctuation spectroscopy as a probe of granular superconducting diamond films

G. M. Klemencic,[1,*] J. M. Fellows,[2] J. M. Werrell,[1] S. Mandal,[1] S. R. Giblin,[1] R. A. Smith,[3] and O. A. Williams[1]
[1]*School of Physics and Astronomy, Cardiff University, Queen's Buildings, The Parade, Cardiff CF24 3AA, United Kingdom*
[2]*School of Physics, H. H. Wills Physics Laboratory, University of Bristol, Tyndall Avenue, Bristol BS8 1TL, United Kingdom*
[3]*School of Physics and Astronomy, University of Birmingham, Edgbaston, Birmingham B15 2TT, United Kingdom*
(Received 22 March 2017; published 6 September 2017)

We present resistance versus temperature data for a series of boron-doped nanocrystalline diamond films. Upon extracting the fluctuation conductivity near the critical temperature we observe three distinct scaling regions—three-dimensional (3D) intragrain, quasi-0D, and 3D intergrain—in confirmation of the prediction of Lerner, Varlamov, and Vinokur. The location of the dimensional crossovers between these scaling regions allows us to determine the tunneling energy and the Thouless energy directly. This is a demonstration of the use of *fluctuation spectroscopy* to determine the properties of a superconducting granular system.

DOI: 10.1103/PhysRevMaterials.1.044801

I. INTRODUCTION

Granular materials offer rich physical systems with which to study the interplay between electron correlations and the mesoscopic effects of disorder. The occurrence of the metal-insulator and superconductor-insulator transitions appear to be strongly linked to granularity, be it structural or pertaining to variations of the order parameter [1–3]. There are also clear theoretical predictions for the signature of granularity in the transport properties of disordered superconductors close to the superconducting transition [4–7]. Boron-doped nanocrystalline diamond (BNCD) provides a suitable tunable material in which to explore these theoretical predictions. Superconductivity was first observed in high-pressure, high-temperature fabricated boron-doped diamond in 2004 [8]. The phenomenon was quickly demonstrated in both single-crystalline [9] and polycrystalline [10] diamonds synthesized by chemical vapor deposition (CVD). While superconductivity in doped semiconductor materials [11,12] is an active area of research, and although nanocrystalline diamond retains many of the desirable mechanical properties of single-crystalline material [13], a sometimes overlooked property in the study of superconductivity in polycrystalline boron-doped diamond is the physical granularity itself.

II. FLUCTUATIONS IN GRANULAR SUPERCONDUCTORS

A clear experimental signature of superconducting granular systems, as pointed out by Lerner, Varlamov, and Vinokur [5] (henceforth referred to as LVV), is that there are three distinct temperature regimes in the vicinity of the critical temperature (T_c), distinguished by the magnitude of the temperature-dependent Ginzburg-Landau coherence length. At temperatures immediately above T_c, short-lived Cooper pairs act as charge carriers, modifying the conductivity. The principal modification close to T_c is the Aslamazov-Larkin pair contribution to the conductivity—the so-called paraconductivity [14]. When the coherence length is much larger than the typical grain size, the granularity is not seen by a Cooper pair and the system behaves as a three-dimensional (3D) superconductor with paraconductivity taking the well-known form $\propto\epsilon^{-1/2}$, where $\epsilon = (T - T_c)/T_c$ is the reduced temperature. When the coherence length is comparable to the typical grain size, each grain acts as its own 0D superconductor for which the paraconductivity is expected to be $\propto\epsilon^{-2}$. However, in addition, the intergrain transport requires two electrons to hop with a Cooper pair lifetime $\propto 1/\epsilon$ such that the conductivity in a quasi-0D (q0D) array of grains should in fact be $\propto\epsilon^{-3}$. Finally, when the coherence length is much smaller than the typical grain size, a Cooper pair moves through the grain as though it were a bulk 3D system so that the conductivity is again $\propto\epsilon^{-1/2}$, albeit reduced by renormalization of the scattering time due to scattering at grain boundaries [15]. Although these scaling laws are presented on physical grounds, they are calculated directly from the appropriate Aslamazov-Larkin diagram in the original LVV paper, accounting for intergrain tunneling; hence the theory is both intuitive and rigorous. Shifting perspective from length scales to reduced temperature scales, the LVV theory predicts a dimensional crossover from 3D to q0D behavior at $\epsilon \sim \epsilon_t = \Gamma/k_B T_c$, where Γ is the tunneling energy, and a second crossover from q0D back to 3D at $\epsilon \sim \epsilon_g = E_{Th}/k_B T_c$, where $E_{Th} = \hbar\mathcal{D}/a^2$ is the Thouless energy, $\mathcal{D}$ is the intragrain diffusion constant, and a is the typical grain size. To summarize, the LVV theory predicts a fluctuation paraconductivity, σ_{fl}, with scaling behavior

$$\frac{d\ln\sigma_{fl}}{d\ln\epsilon} = \begin{cases} -\frac{1}{2} & \text{(3D)} \quad \epsilon \lesssim \epsilon_t, \\ -3 & \text{(q0D)} \quad \epsilon_t \lesssim \epsilon \lesssim \epsilon_g, \\ -\frac{1}{2} & \text{(3D)} \quad \epsilon_g \lesssim \epsilon \lesssim 1. \end{cases} \tag{1}$$

In this paper, by measuring the resistive transition of BNCD films, we experimentally observe a clear signature of granularity due to different regimes of superconducting fluctuation contributions at $T \gtrsim T_c$. To this end, we present a detailed fluctuation spectroscopy analysis of transport measurements on a series of BNCD films with changing grain sizes as controlled by film thickness. We observe the dimensional crossovers with ϵ scaling predicted by the LVV theory, extracting the Thouless energy and tunneling energy directly, while estimating average inter- and intragrain diffusion constants. Further to this observation, we anticipate that the considerable morphological control afforded by the tunable growth of superconducting BNCD [16] provides a rich physical system with which to further test these theoretical models. Dimensional crossovers in superconducting materials have been investigated in the

*Corresponding author: klemencicg@cardiff.ac.uk

 ©2017 American Physical Society

past [17–19] but not used as a method of material characterization. The close agreement between theory and experiment shown here allows the extraction of various physical characteristics of films; this simple method of determining physical parameters should be useful in selecting materials for device applications such as superconducting single photon detectors (SSPDs) and kinetic inductance detectors (KIDs), among others [20–22].

III. CVD-GROWN BORON-DOPED NANOCRYSTALLINE DIAMOND

The exact structural granular morphology of a CVD-grown BNCD film is sensitive to a number of parameters. To efficiently grow a thin uniform film on a nondiamond substrate, the surface must first be populated with a high density of nucleation sites—typically small diamond particles—from which the film's composite grains may grow [23]. The density and initial size of particles are significant factors in the average grain-size distribution of the resultant film, which is formed by the competitive growth of the seed crystals in a plasma comprising a dilute concentration of methane in hydrogen. A hydrogen-rich environment preferentially etches nondiamond material; the grains grow in a columnar structure originating from the particular nucleation sites, and increase in size as the film grows thicker [24]. By changing the ratio of methane and hydrogen in the plasma, larger or smaller grains can be grown, for a lower or higher methane percentage, respectively [25]. In addition to this, CVD allows control of the growth temperature and chamber pressure. All of these parameters, and the interplay between them, determine the granularity of the nanodiamond film.

While intrinsic diamond is a wide-band-gap insulator [26], the incorporation of boron above a critical value, $n_c \sim 4.5 \times 10^{20}$ cm^{-3}, provides the necessary charge carriers for superconductivity [27]. There is some evidence to suggest that boron is incorporated more efficiently in some growth directions than others [28], and that an adjustment of the methane concentration in BNCD growth can affect the overall dopant concentration, leading to the reporting of some contradictory results [24,25]. Given the tunability of CVD diamond growth, it is no surprise that there is a wide variation in the properties of polycrystalline superconducting diamond reported in the literature [10,24,25,27,29–32]. It is exactly this tunability, however, that is potentially a powerful tool in the well-controlled production of this granular superconducting material.

IV. SAMPLE GROWTH AND CHARACTERIZATION

We grew a series of BNCD films on SiO_2-buffered (100) silicon wafers by microwave plasma assisted CVD [33]. Prior to growth, each substrate was seeded by ultrasonic agitation in a monodisperse aqueous colloid of nanodiamond particles approximately 5 nm in diameter. This process has been shown to provide a nucleation site density in excess of 10^{11} cm^2 [23]. The substrates were held at $\sim$720 °C in a dilute gas mixture of methane and trimethylboron in hydrogen, with a 3% methane concentration and a B/C ratio of 12800 ppm, and a chamber pressure and microwave power of 40 Torr and 3.5 kW, respectively. The growth time was varied across the set such that the film thickness was in the range 35–564 nm; the B/C ratio was not changed between samples, thus we expect similar boron concentrations across the series [24].

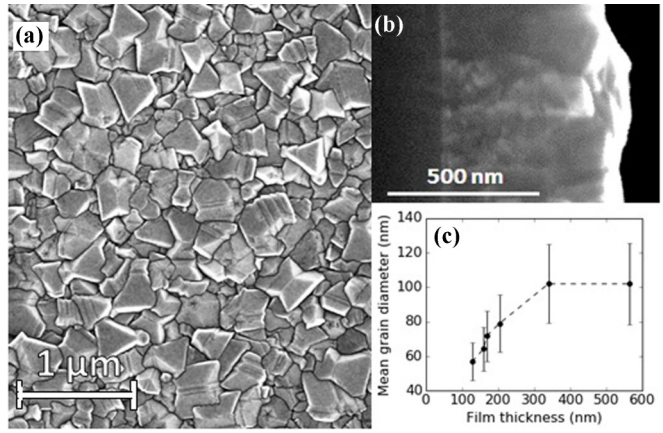

FIG. 1. (a) Surface morphology of 564-nm-thick nanocrystalline diamond film imaged by SEM. (b) The thickness was determined by imaging a cross section of the film. (c) Grain-size analysis gave a measure of the mean grain diameter, shown as a function of film thickness.

Scanning electron microscope (SEM) images were used to quantify the granularity of the BNCD films. As an example, Fig. 1(a) shows the surface morphology of 564-nm-thick film. The polycrystalline nature of the material is evident, with no single dominant growth direction observable. Figure 1(b) shows a cross-sectional image of the same film used to determine the thickness; the columnar grain structure and surface roughness is also evident. The lateral surface grain-size distribution determined from the SEM images was used to give a mean grain diameter as a function of film thickness, shown in Fig. 1(c). It is clear that thicker films have a larger mean grain size, although detailed grain-size analysis revealed that the 339- and 564-nm-thick films have a similar grain-size distribution at the surface. The temperature dependence of the sample resistances, shown in Fig. 2, were measured in the range 2–300 K using a Quantum Design physical property measurement system. Silver paste contacts were made to the sample surface in a four-wire van der Pauw configuration. The $R(T)$ curves in Fig. 2 show an overall increase in T_c as the film thickness is increased; no further change in T_c is observed in thicker samples.

V. RESULTS AND DISCUSSION

A. Extraction of fluctuation conductance

In order to extract the fluctuation contribution to the conductivity, we first subtract the normal-state temperature dependence. The high-temperature conductivity in granular diamond has a pronounced $\sqrt{T}$ behavior, shown in Fig. 3(a), as might be expected for a disordered system with an appreciable electron-electron interaction [34]. This has previously been observed in single-crystal diamond samples [35]. We therefore extract the normal-state contribution by fitting the high-temperature conductance data to $G_{\rm ns} = a + b\sqrt{T}$. The fluctuation conductance in the vicinity of the transition is therefore $G_{\rm fl} = G - G_{\rm ns}$. We determine the transition temperature T_c as

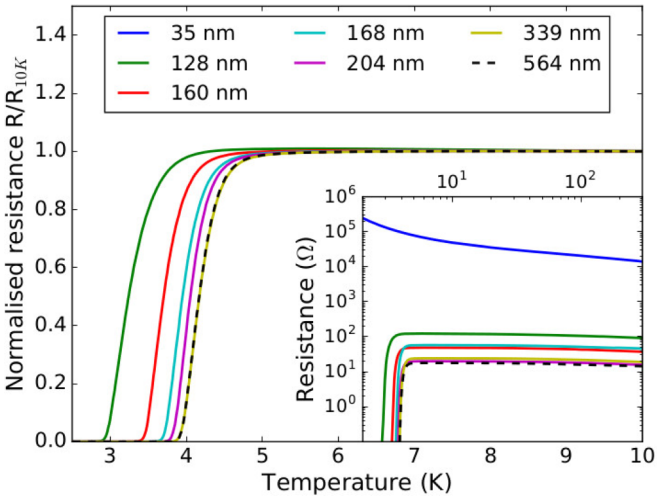

FIG. 2. Resistive transition of thickness-varied series of BNCD films normalized to $R_{10\,\mathrm{K}}$. The thinnest film is omitted due to lack of observable superconductivity in this temperature range. Inset shows $R(T)$ from room temperature to 2 K.

the point at which G_{fl} diverges, shown in Fig. 3(b) as a red vertical line on the $R(T)$ curve for a 564-nm-thick film. This fluctuation analysis is in contrast to the typical experimental procedure of defining T_c as the midpoint of the transition region, but is necessary if we are to correctly assign the reduced temperature. Figure 3(c) shows the fluctuation conductance as a function of the reduced temperature, plotted on a logarithmic scale. The emergence of distinct regions of different scaling behavior is immediately observable, supporting LVV theory. This behavior is observable in every film in the series. Figure 3(c) is representative of the data obtained. Similar results of fluctuation spectroscopy for all films are shown in Figs. 1–6 in the Supplemental Material [36].

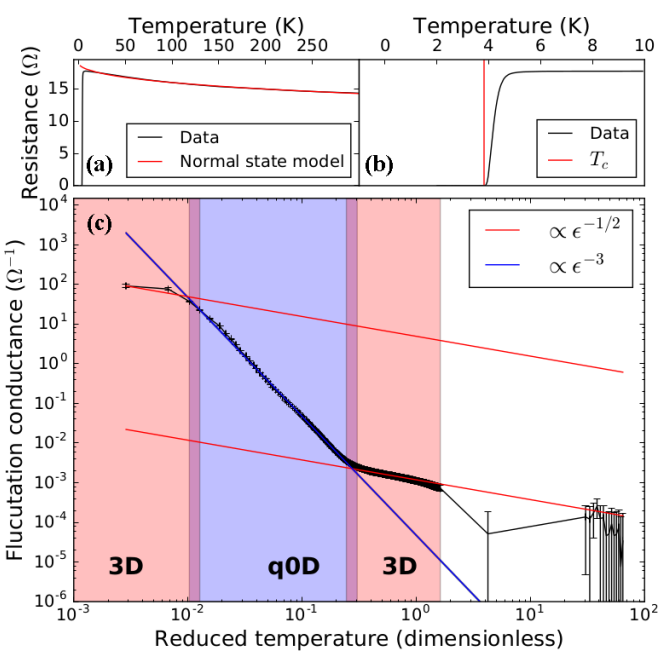

FIG. 3. Fluctuation spectroscopy of 564-nm-thick BNCD film. (a) A fit to the high-temperature region reveals a $T^{0.5}$ dependence, and allows extraction of G_{ns}. (b) T_c is defined as the point at which the conductance diverges, depicted in red. (c) Fluctuation conductance, $G_{\mathrm{fl}} = G - G_{\mathrm{ns}}$, as a function of reduced temperature, $\epsilon = (T - T_c)/T_c$.

B. Material characterization from crossover temperatures

From the distinct temperature regimes observable in the fluctuation conductivity, the Thouless energy E_{Th} and the tunneling energy Γ can immediately be extracted. As the crossover is smooth, one cannot simply find a point at which it occurs. Instead we define a crossover region as that in which two scaling forms can be fit within 10% of the experimental values. We then use the upper and lower boundaries to estimate the error on the crossover point. In Fig. 3(c), the crossover regions found in this manner are shown as the regions where the two shadings overlap. While there are few data points in the dimensional regime immediately following T_c, it is clear that there exists a region with a fluctuation conductance that is quantitatively different for the q0D regime that follows. We note that despite having the fewest points, the scaling behavior in the bulk 3D regime follows the Ginzburg-Landau theory near the transition temperature and as such is expected.

The tunneling and Thouless energies were calculated based on these crossovers for each film. The tunneling energy was extracted from the 3D to the q0D crossover for each sample and an average found to be $\Gamma = 4.2 \pm 2.0\ \mu\mathrm{eV}$. This is the energy associated with charge carriers crossing a grain boundary. In contrast, by definition, the Thouless energy should be proportional to the inverse square of the mean grain size, with the constant of proportionality giving the intragrain diffusion constant. In Fig. 4, the Thouless energy is extracted from the q0D to the 3D crossover for each film, and is plotted as a function of a^{-2}. The shaded region represents the error on the linear fit; it is important to note here that the main contribution to the uncertainty is the grain-size distribution as quantified by SEM image analysis. This result serves as a consistency check of the underpinning physics; the extracted values of

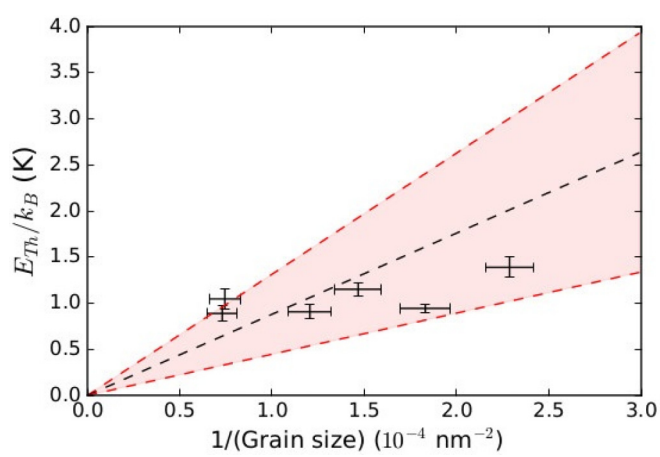

FIG. 4. Thouless energy E_{Th} as a function of $1/a^2$, where a is the mean grain diameter. A linear fit is used to calculate the electron diffusion constant as $\mathcal{D} = 11.5 \pm 5.7\ \mathrm{cm}^2/\mathrm{s}$. The shaded area represents the error on the linear fit due to the grain-size distribution.

E_{Th} fall within the the range given by the spread of grain sizes obtained from SEM analysis, thus demonstrating that our measurement is consistent with the theoretical prediction that describes them. Given the known grain-size distribution of the films, an average of the Thouless energy for all films can be extracted and the intragrain diffusion constant $\mathcal{D}$ is calculated as $11.5 \pm 5.7\ \mathrm{cm}^2/\mathrm{s}$. The bulk diffusion constant for a BNCD film grown under the same conditions was recently measured to be $0.6\ \mathrm{cm}^2/\mathrm{s}$ [37]. If we replace the Thouless energy with the tunneling energy, we obtain the effective intergrain diffusion constant defined as $\mathcal{D}_{\mathrm{eff}} = a^2\Gamma/\hbar$ [4], which we find to be $0.54 \pm 0.36\ \mathrm{cm}^2/\mathrm{s}$. We note the large distribution of grain sizes for all the films as a large source of error and that this analysis does not take into account any effect of the grain-boundary properties, however, we clearly show that this method of extracting physical parameters is consistent with other approaches.

VI. CONCLUSIONS

To conclude, we have applied a theoretical model of the fluctuation paraconductivity in granular superconductors to a series of BNCD films to a series of samples with varying film thickness. We demonstrate an excellent agreement between the LVV theory and experimental measurements of $R(T)$ in BNCD films over a wide temperature range for all samples. The clear observation of dimensional crossover in the fluctuation region allows conclusions to be drawn about the physical influence of the structural granularity of the material. We present a simple method of estimating the tunneling energy and the Thouless energy, leading to an estimate of the inter- and intragrain electron diffusion constants, respectively. Knowledge of these parameters is an important consideration in the design of superconducting electronic devices such as SSPDs or KIDs. We propose that the technique of fluctuation spectroscopy demonstrated here may prove to be a remarkably simple yet valuable tool for characterizing the microscopic properties of BNCD and other granular superconducting materials.

ACKNOWLEDGMENTS

The authors wish to thank A. Papageorgiou for help with image processing. We gratefully acknowledge support by the European Research Council under the EU Consolidator Grant "SUPERNEMS" (Project No. 647471).

[1] V. F. Gantmakher and V. T. Dolgopolov, Phys.-Usp. **53**, 1 (2010).
[2] B. Sacépé, C. Chapelier, T. I. Baturina, V. M. Vinokur, M. R. Baklanov, and M. Sanquer, Phys. Rev. Lett. **101**, 157006 (2008).
[3] H. M. Jaeger, D. B. Haviland, B. G. Orr, and A. M. Goldman, Phys. Rev. B **40**, 182 (1989).
[4] I. Beloborodov, A. Lopatin, V. Vinokur, and K. Efetov, Rev. Mod. Phys. **79**, 469 (2007).
[5] I. V. Lerner, A. A. Varlamov, and V. M. Vinokur, Phys. Rev. Lett. **100**, 117003 (2008).
[6] G. Deutscher, Y. Imry, and L. Gunther, Phys. Rev. B **10**, 4598 (1974).
[7] Y. Imry and M. Strongin, Phys. Rev. B **24**, 6353 (1981).
[8] E. Ekimov, V. Sidorov, E. Bauer, N. Mel'Nik, N. Curro, J. Thompson, and S. Stishov, Nature (London) **428**, 542 (2004).
[9] E. Bustarret, J. Kačmarčik, C. Marcenat, E. Gheeraert, C. Cytermann, J. Marcus, and T. Klein, Phys. Rev. Lett. **93**, 237005 (2004).
[10] Y. Takano, M. Nagao, I. Sakaguchi, M. Tachiki, T. Hatano, K. Kobayashi, H. Umezawa, and H. Kawarada, Appl. Phys. Lett. **85**, 2851 (2004).
[11] X. Blase, E. Bustarret, C. Chapelier, T. Klein, and C. Marcenat, Nat. Mater. **8**, 375 (2009).
[12] E. Bustarret, Phys. C (Amsterdam, Netherlands) **514**, 36 (2015).
[13] O. A. Williams, A. Kriele, J. Hees, M. Wolfer, W. Müller-Sebert, and C. Nebel, Chem. Phys. Lett. **495**, 84 (2010).
[14] A. Larkin and A. Varlamov, *Theory of Fluctuations in Superconductors* (Clarendon Press, Oxford, UK, 2005).
[15] The detailed calculation presented by LVV predicts this power law to be -2 but here we use an argument based on the simple physics of the system to predict a power law of $-1/2$ which is in agreement of our experimental results.
[16] O. A. Williams, Diamond Relat. Mater. **20**, 621 (2011).
[17] X. Xiang, J. Hou, V. H. Crespi, A. Zettl, and M. L. Cohen, Nature (London) **361**, 54 (1993).
[18] G. Deutscher and S. Dodds, Phys. Rev. B **16**, 3936 (1977).
[19] K. Makise, H. Terai, T. Yamashita, S. Miki, Z. Wang, Y. Uzawa, S. Ezaki, T. Odou, and B. Shinozaki, J Phys.: Conf. Ser. **400**, 022064 (2012).
[20] C. M. Natarajan, M. G. Tanner, and R. H. Hadfield, Supercond. Sci. Technol. **25**, 063001 (2012).
[21] P. K. Day, H. G. LeDuc, B. A. Mazin, A. Vayonakis, and J. Zmuidzinas, Nature (London) **425**, 817 (2003).
[22] A. Shurakov, Y. Lobanov, and G. Goltsman, Supercond. Sci. Technol. **29**, 023001 (2015).
[23] O. A. Williams, O. Douhéret, M. Daenen, K. Haenen, E. Ōsawa, and M. Takahashi, Chem. Phys. Lett. **445**, 255 (2007).
[24] B. Willems, G. Zhang, J. Vanacken, V. Moshchalkov, S. Janssens, K. Haenen, and P. Wagner, J. Phys. D: Appl. Phys. **43**, 374019 (2010).
[25] G. Zhang, S. Janssens, J. Vanacken, M. Timmermans, J. Vacík, G. Ataklti, W. Decelle, W. Gillijns, B. Goderis, K. Haenen *et al.*, Phys. Rev. B **84**, 214517 (2011).
[26] F. Celii and J. Butler, Annu. Rev. Phys. Chem. **42**, 643 (1991).
[27] T. Klein, P. Achatz, J. Kacmarcik, C. Marcenat, F. Gustafsson, J. Marcus, E. Bustarret, J. Pernot, F. Omnes, B. E. Sernelius *et al.*, Phys. Rev. B **75**, 165313 (2007).
[28] K. Ushizawa, K. Watanabe, T. Ando, I. Sakaguchi, M. Nishitani-Gamo, Y. Sato, and H. Kanda, Diamond Relat. Mater. **7**, 1719 (1998).
[29] E. Bustarret, Phys. Status Solidi A **205**, 997 (2008).
[30] P. Achatz, W. Gajewski, E. Bustarret, C. Marcenat, R. Piquerel, C. Chapelier, T. Dubouchet, O. Williams, K. Haenen, J. A. Garrido *et al.*, Phys. Rev. B **79**, 201203 (2009).
[31] F. Dahlem, P. Achatz, O. A. Williams, D. Araujo, E. Bustarret, and H. Courtois, Phys. Rev. B **82**, 033306 (2010).

[32] W. Gajewski, P. Achatz, O. A. Williams, K. Haenen, E. Bustarret, M. Stutzmann, and J. A. Garrido, Phys. Rev. B **79**, 045206 (2009).

[33] O. A. Williams, M. Nesladek, M. Daenen, S. Michaelson, A. Hoffman, E. Osawa, K. Haenen, and R. Jackman, Diamond Relat. Mater. **17**, 1080 (2008).

[34] B. Altshuler and A. Aronov, *Electron-Electron Interaction in Disordered Conductors*, edited by A. L. Efros and M. Pollak (Elsevier, Amsterdam, 1985).

[35] J. Bousquet, T. Klein, M. Solana, L. Saminadayar, C. Marcenat, and E. Bustarret, Phys. Rev. B **95**, 161301 (2017).

[36] See Supplemental Material at http://link.aps.org/supplemental/10.1103/PhysRevMaterials.1.044801 for equivalent analysis of additional samples.

[37] N. Titova, A. I. Kardakova, N. Tovpeko, S. Ryabchun, S. Mandal, D. Morozov, G. M. Klemencic, S. R. Giblin, O. A. Williams, G. N. Goltsman, and T. M. Klapwijk, IEEE Trans. Appl. Supercond. **27**, 1 (2017).